

## Picosecond studies of energy transfer of donor and acceptor dye molecules in solution. II. A concentration dependence

P. Y. Lu, Z. X. Yu, R. R. Alfano, and J. I. Gersten

*Institute of Ultrafast Spectroscopy and Lasers, Physics Department, The City College of New York, New York, New York 10031*

(Received 16 November 1982)

The energy transfer between donor and acceptor molecules has been studied by steady-state and picosecond time-resolved spectroscopies in solutions with a given concentration of donor molecules and different concentrations of acceptor molecules. The rise and decay times of the fluorescence from donor and acceptor molecules were measured. The decrease of the decay times of the donors and the rise time of the acceptors with an increase of the concentration of acceptors observed in the mixed solution indicates a faster energy-transfer rate between the donors and acceptors. Theoretically calculated fluorescence profiles and efficiencies of energy transfer are in agreement with the experimental results.

### INTRODUCTION

Dyes are sensitized by light and are good materials for many industrial applications. Understanding the physical processes associated with photoexcited dyes is important for the efficient conversion and transfer of optical energy to other spectral regions. The photoexcitation of a solution with two kinds of dyes has been used to study the optical energy transfer<sup>1-15</sup> between donor and acceptor molecules. Theories<sup>16-23</sup> have been developed to explain the possible mechanism of energy transfer in mixed dyes. However, there are few experimental measurements which studied both the kinetics of the donor and acceptor molecules simultaneously. Recently,<sup>24</sup> we have measured the rise and decay of the fluorescence profiles of the donor and acceptor molecules in a mixed solution at a fixed concentration ( $2.5 \times 10^{-3} M$ ). A theoretical model was formulated to fit the experimental results for the time-resolved fluorescence profiles of the donor and acceptor molecules. The consistency of the theory with the experimental data<sup>24</sup> has given some of the conditions for efficient energy transfer between the donor and acceptor dye molecules. In order to obtain additional information on the energy-transfer mechanisms and transfer efficiency, a series of measurements with different concentrations of donor and acceptor molecules are necessary.

In this paper, experimental measurements and theoretical calculations were performed on mixed solutions of a fixed concentration of donor molecules with different concentrations of acceptor molecules for the following pair of dyes: (1) Rhodamine-6G (the donor) and Oxazine-4 per-

chlorate (the acceptor), and (2) Rhodamine-B (the donor) and Nile Blue A perchlorate (the acceptor). This is a continuation of the research presented in Ref. 24. The dyes were dissolved in ethylene glycol at room temperature where diffusion is small and neglected.

### THEORY

The fluorescence intensity per unit volume from the donor and acceptor molecules as function of time were formulated by us and are presented in

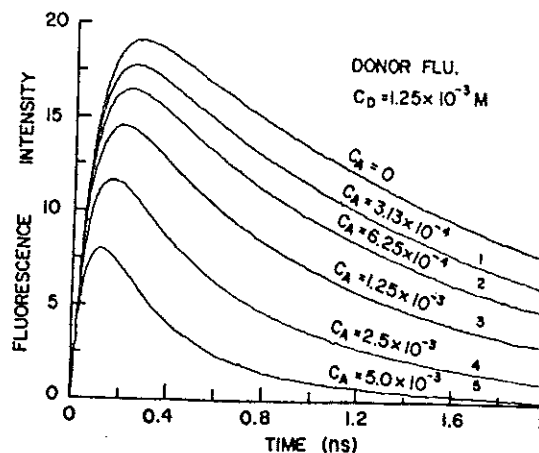


FIG. 1. Theoretical calculation of the fluorescence profiles vs time obtained by Eq. (9) of Ref. 24 for the donor at concentration  $1.25 \times 10^{-3} M$  and various concentrations of acceptors. Detection system rise time is assumed to be 80 ps considering the convolution of the signal and streak camera. Critical transfer distance  $R_0$  is assumed to be 55 Å. Ratio of absorption cross section of donor to acceptor is 22. Decay time of donor is 1.85 ns.

Ref. 24. Using Eqs. (9) and (11) in Ref. 24, the fluorescence profiles versus time were calculated numerically for a given concentration ( $1.25 \times 10^{-3} M$ ) of the donor mixed with various concentrations of acceptors. The calculated fluorescence profiles in time of the donor and acceptor molecules are displayed in Figs. 1 and 2. In Fig. 1, the fluorescence intensity and quantum yield of the donor decreases as the concentration of acceptor increases. In Fig. 2, the fluorescence intensity and quantum

yield of the acceptor increases as the concentration of the acceptor increases. This implies a larger and more efficient energy transfer in the higher concentration of acceptor molecules because there are more acceptor molecules surrounding a given donor molecule. The mean distance between the acceptor and donor is smaller than critical energy-transfer distance  $R_0$  for higher energy transfer.

According to the theoretical model,<sup>24</sup> the efficiency of the energy transfer  $\eta_E$ , is defined as follows:

$$\eta_E = 1 - \frac{\int_0^\infty \int_0^t \exp[-\rho_D(t-\tau) - g_D\tau - (4\pi/3)\eta_A \sqrt{\pi \Delta\tau}] d\tau dt}{\int_0^\infty \int_0^t \exp[-\rho_D(t-\tau) - g_D\tau] d\tau dt} \quad (1)$$

where the parameters are defined in Ref. 24. On the other hand, the efficiency of energy transfer at average distance between donor and acceptor can be written as

$$\eta_R = \frac{k_{ET}}{k_{ET} + g_D} = \frac{\tau_D^{-1}(R_0/\bar{R})^6}{\tau_D^{-1}(R_0/\bar{R})^6 + \tau_D^{-1}} = \frac{(R_0/\bar{R})^6}{1 + (R_0/\bar{R}_c)^6} \quad (2)$$

where  $k_{ET}$  is the average energy-transfer rate and  $R_0$  is the actual energy-transfer distance for the donor and acceptor.<sup>24</sup> The value of  $\eta_E$  can be used to check the consistency of the theoretical calculation by comparing the results obtained from Eqs. (1) and

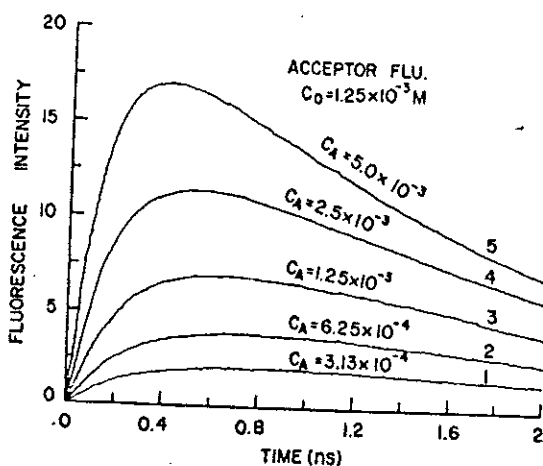


FIG. 2. Theoretical calculation of the fluorescence profiles vs time obtained by Eq. (11) of Ref. 24 for the acceptor at various concentrations and the donor at a concentration of  $1.25 \times 10^{-3} M$ . System response function is 80 ps. Decay times of donor and acceptor are assumed to be 1.85 and 1.45 ns, respectively. Critical transfer distance is 55 Å. Ratio of the absorption cross section of donor to acceptor is 22.

(2) with the experimental measurements for the different concentrations of acceptors mixed with a fixed quantity of donors.

#### EXPERIMENTAL SETUP

The steady-state luminescence spectra were measured using a conventional method. Light at 530 nm was chopped and focused frontally onto the sample. The fluorescence signal from the sample was focused onto the slit of a Spex double  $\frac{1}{2}$ -m spectrometer, detected by an RCA 7265 photomultiplier and measured by a lock-in amplifier combination. The fluorescence spectrum was recorded on an X-Y recorder.

The experimental setup used in picosecond time-resolved studies was described previously.<sup>24</sup> The laser system<sup>25</sup> consisted of an Nd:phosphate glass oscillator and amplifier which provides a 6-ps, 1054-nm laser pulse. A single pulse was frequency doubled by a second harmonic generator, KDP (potassium dihydrogen phosphate). The 527-nm single pulse was delayed by an optical delay device (white cell), collimated, and imaged onto the sample. The Corning 3-67 filters were used to spectrally isolate the fluorescence from the sample. In addition, a Cyan dichroic filter was used to separate the fluorescence component of Rh6G and Hoya R-66 filters were used to isolate the fluorescence component of Oxazine-4 perchlorate. A short pass filter (Ditric, Mass.) at 620 nm was used to separate the fluorescence component of Rhodamine B and a Hoya R-68 filter was used to isolate the component of Nile Blue A perchlorate. A Hamamatsu streak camera<sup>26</sup> (C979) was used to measure the time-resolved fluorescence signals. The fluorescence was collected by lenses and focused onto the slit of the streak camera. The streaked image was digitized by a SIT (silicon intensified target) camera and displayed on the screen of Hamamatsu temporal

analyzer. The overall resolution of detection system is 80 ps on the full time scale of 3.1 ns. The system response for a 6-ps laser pulse is about 80 ps which is the convolution of the laser pulse signal and the streak camera system's response function on the 3.1-ns scale. On the fastest sweep rate of a 400-ps total time display, the streak camera has a resolution of less than 10 ps. The streak camera was focused for the spectral region from 530 to 750 nm. A portion of the 530-nm excitation pulse was directed into the streak camera as a marker prepulse. The absolute zero time point of the fluorescence was found by measuring the time separation between the prepulse and the scattered excitation light from the surface of the sample. A Digital Equipment Corporation Minc 11 minicomputer was used to store the data and correct the streak rate and intensity. A Digital Equipment Corporation PDP10 computer was interfaced with a Minc 11 minicomputer for the analysis of data. Standard numerical methods including scientific subroutines were used in the data analysis and curve fitting. The value for  $R_0$  was determined using the method of minimum standard deviation fitting of the theoretical expressions<sup>24</sup> to the measured intensity time profiles and calculated from the spectral overlap between the absorption and fluorescence spectra for the donor and acceptor pairs. The uncertainty in  $R_0$  was determined from the errors in the calculation and measurements of

the absorption and fluorescence spectral overlap. This increases the minimum standard deviation of the intensity versus time profiles fitting by about 5%.

### SAMPLES

Laser-grade dyes from the Eastman Kodak Company were dissolved in ethylene glycol without further purification. Binary mixtures of donors at  $1.25 \times 10^{-3} M$  and acceptors at various concentrations from  $5 \times 10^{-3} M$  to  $3.13 \times 10^{-4} M$  were prepared. The average distance  $\bar{R}$  between the donor-acceptor molecules in these solutions varied from 40 to 63.5 Å. The mean distance  $\bar{R}^{DD}$  between the donor-donor molecules is 68 Å. The value of the critical transfer distance  $R_0^{DA}$  calculated from the spectroscopic data of the fluorescence spectrum of donors and the absorption spectrum of acceptors are  $56 \pm 1.1$  Å and  $54 \pm 2$  Å for the pair of Rhodamine-6G—Oxazine-4 perchlorate (Rh6G-Ox) and Rhodamine-B—Nile Blue A perchlorate (RhB-NB), respectively. The solutions were contained in a 1- or 2-mm optical path cuvette. The ratio of absorption cross sections  $\beta$  at  $\lambda = 530$  nm for Rhodamine-6G to that of Oxazine-4 perchlorate, and Rhodamine-B to that of Nile Blue A perchlorate were measured to be 22 and 17.5, respectively. At these high absorption ratios, there will be very little direct pumping of the acceptor by the laser.

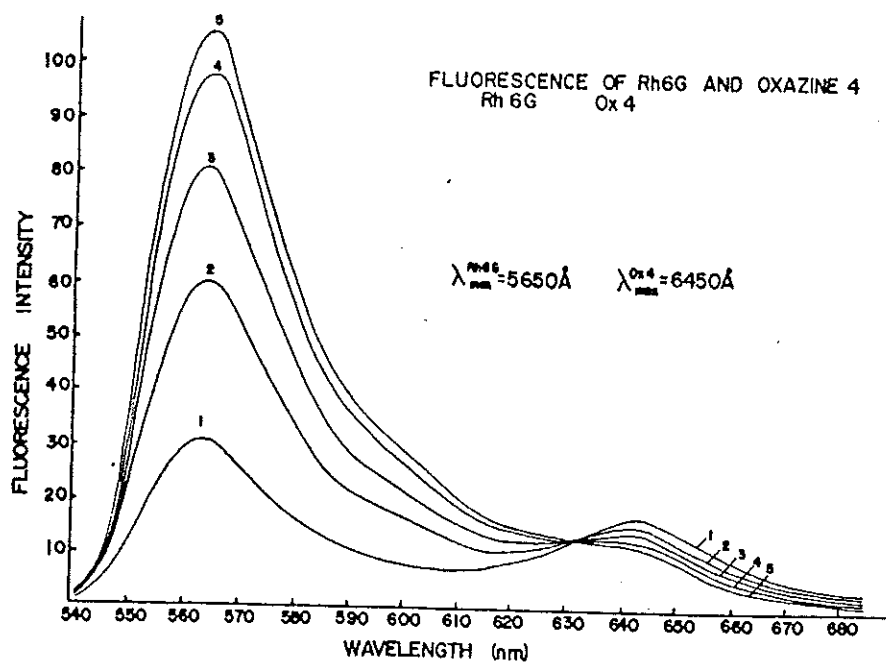


FIG. 3. Experimental measurement of the fluorescence spectra from 540 to 690 nm for Rhodamine-6G (the donor) at a concentration of  $1.25 \times 10^{-3} M$  and Oxazine-4 perchlorate (the acceptor) at various concentrations in ethylene glycol. Peak intensity of Rh6G and Ox4 occurs at 565 and 650 nm, respectively. Acceptor concentrations of Ox4: (1)  $1 \times 10^{-2} M$ ; (2)  $5 \times 10^{-3} M$ ; (3)  $2.5 \times 10^{-3} M$ ; (4)  $1.25 \times 10^{-3} M$ ; (5)  $6.25 \times 10^{-4} M$ .

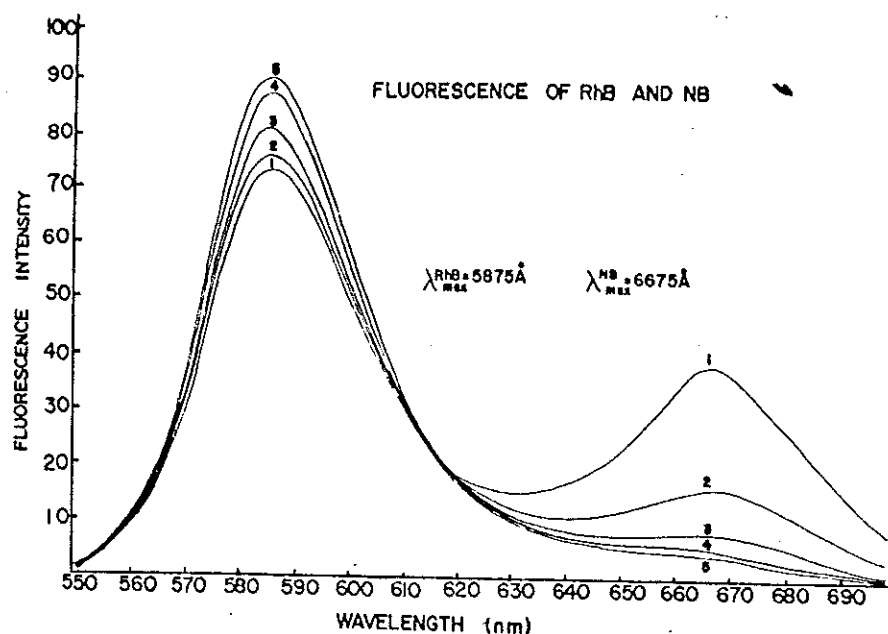


FIG. 4. Experimental measurement of the fluorescence spectra from 550 to 690 nm for Rhodamine-B (the donor) at a concentration of  $1.25 \times 10^{-3} M$  and Nile Blue A perchlorate (the acceptor) at various concentrations in ethylene glycol. Peak intensity of RhB and NB occurs at 588 and 670 nm, respectively. NB concentrations: (1)  $1 \times 10^{-2} M$ ; (2)  $5 \times 10^{-3} M$ ; (3)  $2.5 \times 10^{-3} M$ ; (4)  $1.25 \times 10^{-3} M$ ; (5)  $6.25 \times 10^{-3} M$ .

### EXPERIMENTAL RESULTS

The experimental results are divided into two subsections: (1) Steady-state measurements and (2) time-resolved measurements.

#### Steady-state measurements

The fluorescence spectra of solutions composed of Rhodamine-6G (the donor) at a fixed concentration  $1.25 \times 10^{-3} M$ , mixed with Oxazine-4 perchlorate in ethylene glycol at different concentrations are shown in Fig. 3. The results of the binary mixed solution of Rhodamine-B and Nile Blue A perchlorate are shown in Fig. 4. From data displayed in Figs. 3 and 4 it is clear that when the concentration of the ac-

ceptors is increased there is a decrease of the fluorescence yield of the donors and a corresponding increase in the fluorescence yield of the acceptors. We have observed an increase in the fluorescence intensity and quantum yield of the acceptors in the presence of the donor molecules in the binary solution. This is expected if long-range energy transfer from the donors to acceptors is operative.

#### Time-resolved measurements

Representative time-resolved fluorescence profiles of the donor and acceptor molecules in binary mixtures of Rh6G-Ox and RhB-NB are shown in Figs. 5 and 6, respectively. The theoretical fitting of the profiles by equations in Ref. 24 to the experimental

TABLE I. Energy-transfer efficiency between the donor (Rh6G) and the acceptor (Ox4) in different concentration solutions. Symbols refer to Fig. 11.

Concentration $C_D = 1.25 \times 10^{-3} M$ $C_A$	Experiment result, O (%)	Energy-transfer efficiency ( $\eta_E$ )	
		Calculated by Eq. (1), ● (%)	Calculated by Eq. (2), Δ (%)
$3.13 \times 10^{-4} M$	$16.4 \pm 3$	16.5	30
$6.25 \times 10^{-4} M$	$27.2 \pm 3$	31.0	39
$1.25 \times 10^{-3} M$	$47.7 \pm 6$	52.0	53
$2.5 \times 10^{-3} M$	$72.0 \pm 7$	68.0	71
$5.0 \times 10^{-3} M$	$81.5 \pm 9$	88.0	87

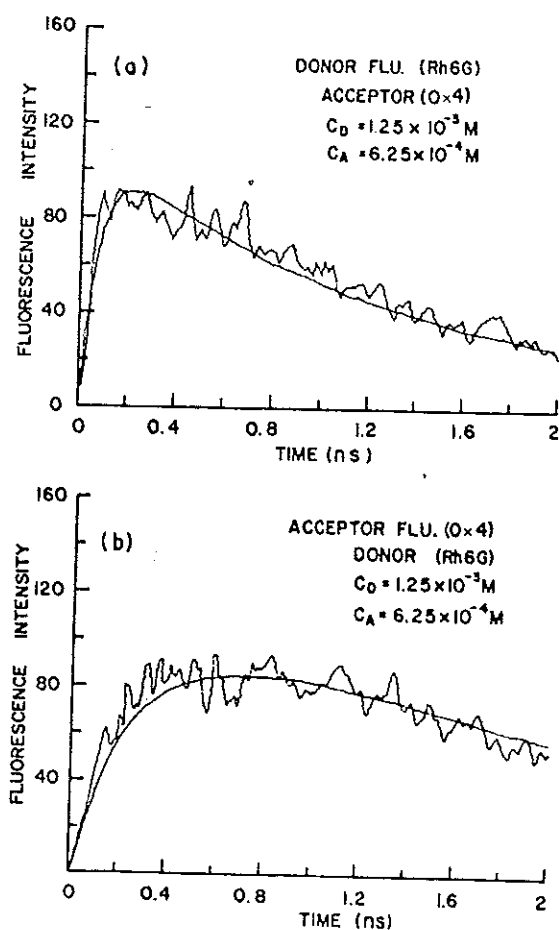


FIG. 5. Experimental measurement of time-resolved fluorescence profile of (a) Rhodamine-6G ( $530 \text{ nm} < \lambda < 600 \text{ nm}$ ) and (b) Oxazine-4 ( $\lambda > 660 \text{ nm}$ ) at a concentration of  $1.25 \times 10^{-3} M$  mixed with Oxazine-4 perchlorate at  $6.25 \times 10^{-4} M$  in ethylene glycol. Filters used are Corning 3-67 and Cyan Dichroic filters. Measurement is fitted by a solid line. Parameters used to fit the data are the system rise time of 80 ps, the critical distance  $R_0 = 55 \text{ \AA}$ , the absorption ratio  $\beta = 22$ , the fluorescence decay time 1.82 ns for Rh6G, and fluorescence decay time of 1.5 ns for neat Ox4 at the respective concentration.

data in Figs. 5 and 6 are shown by the solid lines. The fitting is excellent. The parameters  $R_0$  used in the fittings are  $55 \pm 1 \text{ \AA}$  and  $48 \pm 2 \text{ \AA}$  for the pairs Rh6G and Ox4 and RhB and NB, respectively.

The rise time of fluorescence of Rhodamine-6G is too fast to be resolved<sup>27</sup> [see Fig. 7(a)]. Basically, the observed "rise time" of the time-resolved fluorescence profile of the donor reflects the system response function of the detection system on the 3.1-ns time scale. The slope of the beginning portion of the time-resolved fluorescence profile of donors mixed with various concentrations of acceptors appears steep. This means that the donor in the different acceptor concentrations has a similar ten-

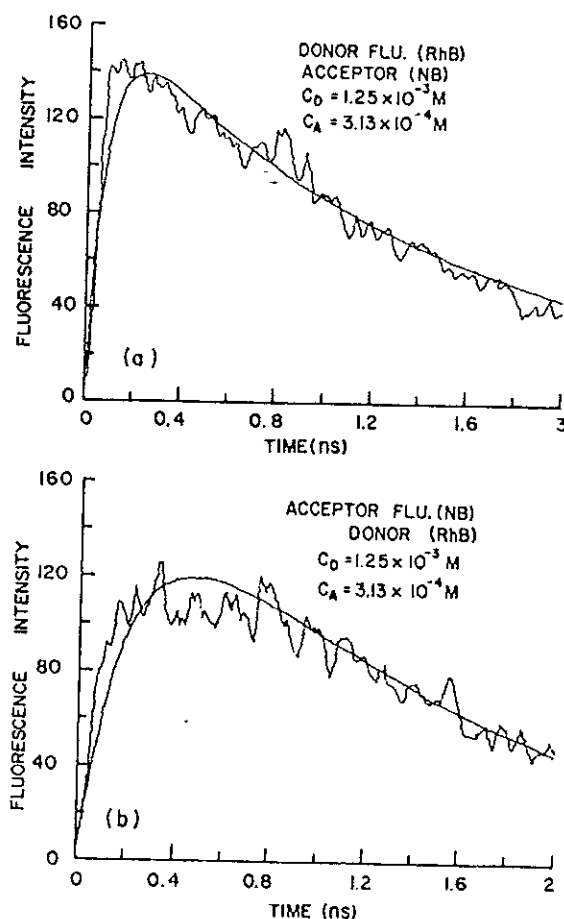


FIG. 6. Experimental measurement of fluorescence profiles of (a) Rhodamine-B ( $530 \text{ nm} < \lambda < 620 \text{ nm}$ ) and (b) Nile Blue A perchlorate ( $\lambda > 680 \text{ nm}$ ) at a concentration of  $1.25 \times 10^{-3} M$  mixed with Nile Blue A perchlorate at concentrations  $3.13 \times 10^{-4} M$  in ethylene glycol. Filters used are a Corning 3-67 and a Ditic short pass filter at 620 nm. Measurements are fitted by a solid line. Parameters used to fit the data are the system rise time of 80 ps, the critical distance  $R_0 = 48 \text{ \AA}$ , the absorption ratio  $\beta = 17.5$ , the fluorescence decay time 1.62 ns for RhB, and fluorescence decay times of 0.77 ns for neat Nile Blue A perchlorate.

dency to be pumped by the laser. The reason that the peak of fluorescence profile of the donors shifts a little in the mixtures with diluted concentrations of acceptors is because of the longer decay time of donor occurring in these cases.

The decay time is defined as the time period between the peak intensity and its  $1/e$  value. In Fig. 7(b), the decay times for the fluorescence profile of Rh6G (donor) in the solution with different concentrations of acceptors are found to decrease as the concentration of Ox4 (acceptor) increases. This decrease occurs because there is more energy transferred to the acceptor molecules surrounding

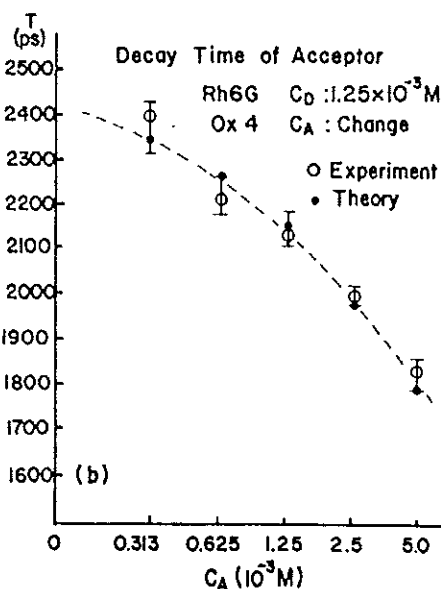
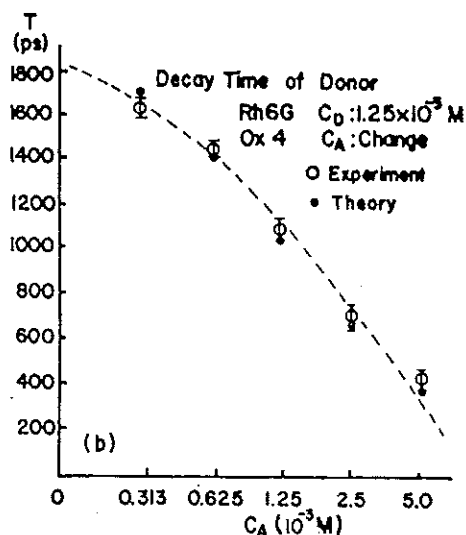
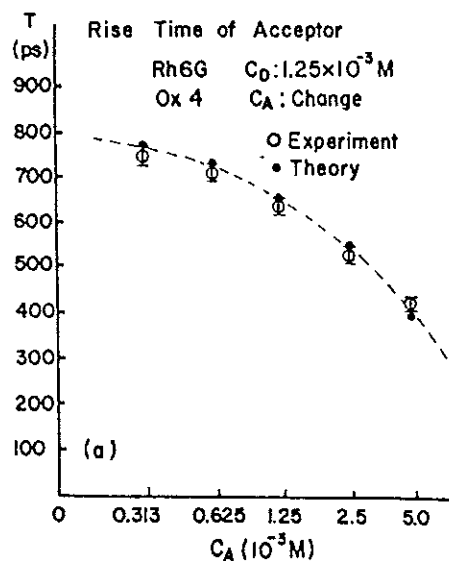
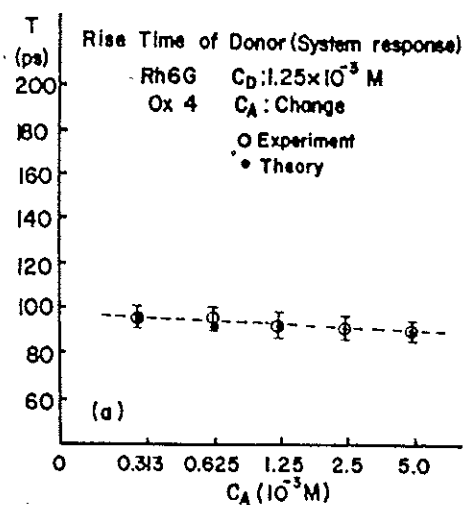


FIG. 7. Observed rise time of the donor (Rh6G) at  $1.25 \times 10^{-3} M$  mixed with various concentrations of acceptor (Ox4). This rise time only reflects the system response time ( $\sim 80$  ps on the 3.1 time scale). (b) ○: Experimental measurement of decay time ( $1/e$  time) of fluorescence profile of Rhodamine-6G at a concentration of  $1.25 \times 10^{-3} M$  mixed with Oxazine-4 perchlorate at different concentrations from  $3.13 \times 10^{-4} M$  to  $5 \times 10^{-3} M$  in ethylene glycol. ●: Decay time deduced from the theoretical fitting curves.

FIG. 8. ○: Experimental measurement of time separation between the peak intensity and starting point of the fluorescence profile of Oxazine-4 perchlorate at different concentrations from  $3.13 \times 10^{-4} M$  to  $5 \times 10^{-3} M$  mixed with Rhodamine-6G at a concentration of  $1.25 \times 10^{-3} M$ . ●: Time separation between the peak intensity and starting point of the theoretical fitting curve. (b) ○: Experimental measurement of decay time of fluorescence profiles of Oxazine-4 perchlorate at different concentrations from  $3.13 \times 10^{-4} M$  to  $5 \times 10^{-3} M$  mixed with Rhodamine-6G at a concentration of  $1.25 \times 10^{-3} M$  in ethylene glycol. ●: Decay time deduced from the theoretical curves.

the donor molecule. At the higher concentration, the average distance between molecules becomes shorter and below  $R_0^{DA}$ . Therefore, there is more efficient long-range energy transfer. This causes a faster decay of the excited electronic state of donor molecules. The time separation between the peak intensity and the starting point of the fluorescence profile of the acceptors becomes much longer than that in the neat solution of acceptors. In Fig. 8(a), the rise time of the peak intensity of the fluores-

cence profile of Ox4 (acceptor) is more than 400 ps in the mixed solution, which is much longer than the rise time of Ox4 in the neat solution of 80 ps (the response time). The time separation of peak in-

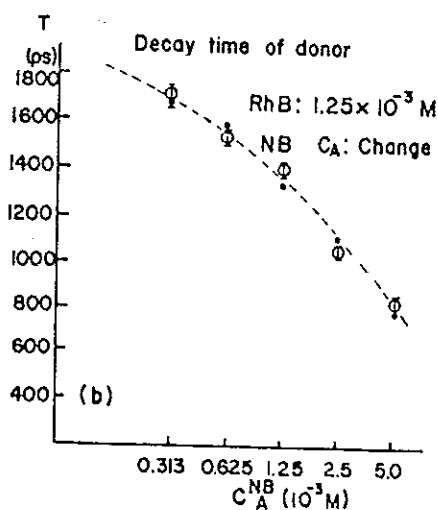
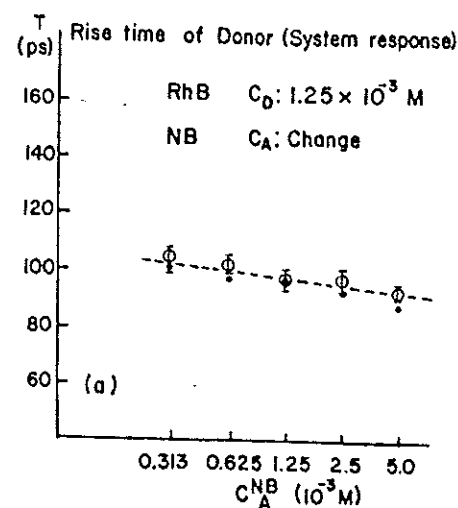


FIG. 9. (a) Observed rise time of the donor (RhB) at  $1.25 \times 10^{-3} M$  mixed with various concentrations of the acceptor (NB). This rise time reflects the system response time ( $\sim 80$  ps). (b)  $\circ$ : Experimental measurement of decay time ( $1/e$  time) of fluorescence profile of RhB at a concentration of  $1.25 \times 10^{-3} M$  mixed with NB at different concentrations from  $3.13 \times 10^{-4} M$  to  $5 \times 10^{-3} M$  in ethylene glycol.

tensity of the fluorescence profile of the acceptor has a tendency to become even longer in the diluted concentration of acceptors. This arises from reduction in the energy transfer from the donor to the acceptor in the diluted case of acceptor in comparison to a faster long-range energy transfer in the concentrated case of acceptor. Overall, the decay time ( $1/e$  time) of the fluorescence profile of Ox4 (acceptor) in the binary mixture is longer than that of Ox4 (1.5 ns) in the neat solution. This is shown in Fig. 8(b). The increased decay time occurs because the donor acts as an energy source which pumps the acceptor molecules causing them to emit longer. According

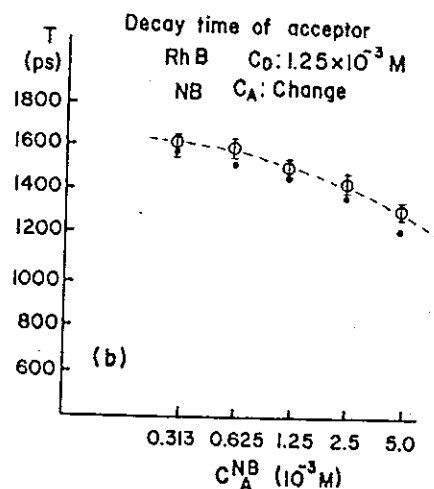
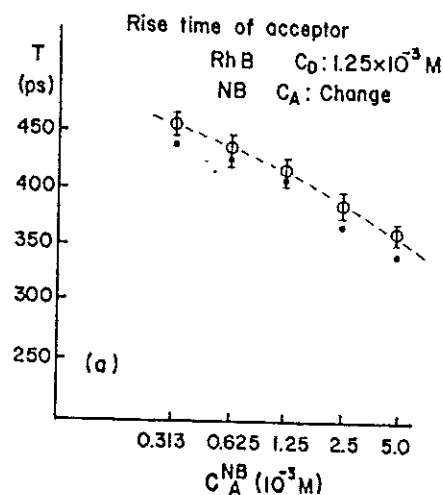


FIG. 10. (a)  $\circ$ : Experimental measurement of time separation of the peak intensity of the fluorescence profile of NB at different concentrations from  $3.13 \times 10^{-4}$  to  $5 \times 10^{-3} M$  mixed with RhB at a concentration of  $1.25 \times 10^{-3} M$ .  $\bullet$ : Time separation of the peak intensity of the theoretical fitting curves. (b)  $\circ$ : Experimental measurement of the decay time of the fluorescence profiles of NB at different concentrations from  $3.13 \times 10^{-4} M$  to  $5 \times 10^{-3} M$  mixed with RhB at a concentration of  $1.25 \times 10^{-3} M$  in ethylene glycol.  $\bullet$ : Decay time deduced from the theoretical curves.

to concentration quenching, the decay time decreases as the concentration increases. Similar results are shown in Figs. 9 and 10 for the binary mixture of Rhodamine-B and Nile Blue A perchlorate.

The efficiency of long-range energy transfer determined by Eqs. (1) and (2) are displayed in Tables I and II for Rhodamine-6G—Oxazine-4 perchlorate and Rhodamine-B—Nile Blue A perchlorate, respectively. The experimental results of the energy-transfer efficiency are also included in Tables I and II for Rh6G-Ox4 and RhB-NB, respectively. These

TABLE II. Energy-transfer efficiency between the donor (RhB) and the acceptor (NB) in different concentration solutions. Symbols refer to Fig. 12.

Concentration $C_D = 1.2 \times 10^{-3} M$ $C_A$	Experiment result, $\circ$ (%)	Energy-transfer efficiency ( $\eta_E$ )	
		Calculated by Eq. (1), $\bullet$ (%)	Calculated by Eq. (2), $\Delta$ (%)
$3.13 \times 10^{-4} M$	$15 \pm 4$	14.7	15.7
$6.25 \times 10^{-4} M$	$20 \pm 1$	24.6	21.6
$1.25 \times 10^{-3} M$	$41 \pm 5$	40.4	33.1
$2.5 \times 10^{-3} M$	$64 \pm 4$	61.2	52.2
$5.0 \times 10^{-3} M$	$81 \pm 6$	80.98	75.4

values are plotted in Figs. 11 and 12. We find that the theoretical model we developed [Eq. (1)] is in better agreement with the experimental data than those obtained from the Forster version given by Eq. (2) for an average energy-transfer distance due to the Forster mechanism.

The value of  $R_0^{DA}$  in the pair of Rh6G-Ox4 (55 Å) is larger than that of the pair of RhB-NB (48 Å). Accordingly, the estimation of  $\eta_E$  by Eq. (2) is a little larger in the diluted concentration case of acceptor for the pair of Rh6G-Ox4 and is a little smaller in the concentrated concentration case of acceptor for the pair RhB-NB. If we define  $R_0$  to be the critical distance at which there is 50% efficiency of energy transfer by Eq. (2), then the values of  $R_0^{DA}$  evaluated from Figs. 11 and 12 are 54.1 and 49.5 Å for Rh6G-Ox4 and RhB-NB, respectively. These

values are close to the values of  $R_0$  obtained from curve fitting, which are 55 and 48 Å, respectively.

## DISCUSSION

The steady-state fluorescence spectra of the binary mixture solution of the donor at a fixed concentration and acceptors at various concentrations were measured. The picosecond time-resolved fluorescence profiles for donor and acceptor molecules were measured by a picosecond laser pulse excitation and streak camera detection system. The rise times and decay time of the donor and acceptor molecules were determined for the different mixtures. A comparison of these times from calculated values fits well for different concentrations of acceptors. The energy-transfer efficiency was measured and calcu-

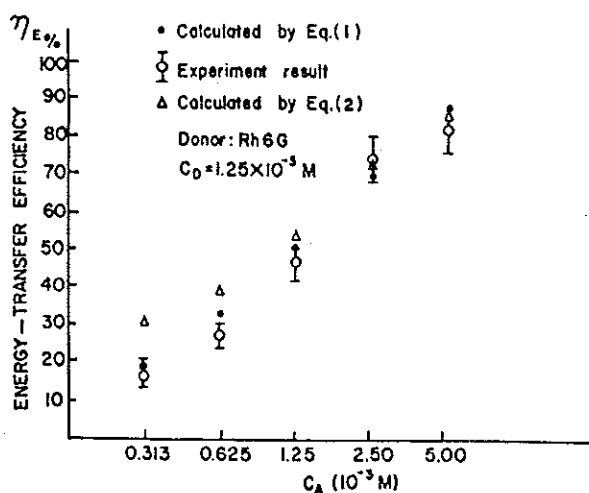


FIG. 11.  $\circ$ : Experimental measurements of the efficiency of long-range energy transfer for Rh6G and Ox4 in different concentrations.  $\bullet$ : Theoretical calculations of the efficiency of energy transfer by Eq. (1).  $\Delta$ : Theoretical estimations of the efficiency of energy transfer by Eq. (2).

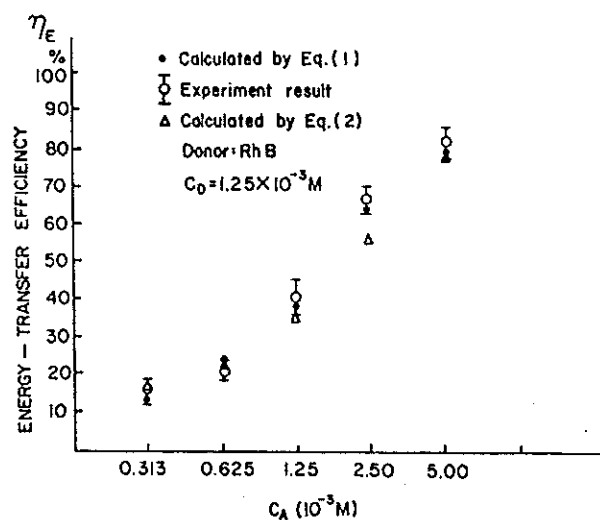


FIG. 12.  $\circ$ : Experimental measurement of the efficiency of long-range energy transfer for RhB and NB in different concentrations.  $\bullet$ : Theoretical calculation of the efficiency of energy transfer by Eq. (1).  $\Delta$ : Theoretical estimation of efficiency of energy transfer by Eq. (2).



lated. The data are in excellent agreement with our theory for the spatial average over the distance between acceptor and donor molecules in the theoretical expressions given for  $D(t)$ ,  $A(t)$ , and  $\eta_E$ . We found that the higher efficiency of energy transfer occurs when the donor and acceptor molecules become close enough so that  $\bar{R}^{DA} < R_0^{DA}$ . Physically, this is due to the stronger long-range interaction between the donor and acceptor molecules in the higher concentration cases. In addition, efficient energy transfer occurs when there is more overlapping of the emission spectrum of the donor and the absorption spectrum of the acceptor. The theoretical fitting parameters  $R_0$  for each case are the same values used in the previous paper.<sup>24</sup> The theoretical model presented in the previous paper<sup>24</sup> [Eqs. (9) and (11)] fits the data well for the various concentrations. The concentration dependence in the spatial average calculation is involved in the argument of the exponential term in Eq. (1). Thus, the efficiency of transfer calculated by Eq. (1) is more accurate and closer to real value than Eq. (2). However, in Eq. (2) the concentration dependence is given by the mean distance  $\bar{R}$  between the molecules.

To check the possibility of a long-range energy transfer between donors,<sup>15</sup> a solution, in the condition for which the donor-donor transfer dominates over donor-acceptor transfer, was prepared with a high concentration of the Rh6G (donor) at  $5 \times 10^{-3} M$  mixed with a low concentration of the Ox4 (acceptor) at  $1.25 \times 10^{-5} M$ . The Ox4 acceptor was supposed to probe the  $D-D$  transfer. Unfortunately, the fluorescence of the acceptor was so weak that no signal was detected at all. The fluorescence of donor in the binary mixture solution in this case is similar to that in the neat solution at the same concentration  $5 \times 10^{-3} M$ . As we pointed out in the previous paper,<sup>24</sup> we chose the pair of donor and acceptor to enhance the long-range energy transfer and to reduce the possibility of  $D-D$  transfer to a negligible value. Since the absorption of laser beam by the donor molecule is large and the critical transfer distance  $R_0^{DA}$  for a donor-acceptor pair is

larger than critical distance  $R_0^{DD}$  for a donor-donor pair and  $R_0^{DD} < \bar{R}^{DD}$ , we conclude that the donor-donor energy transfer is negligible in samples in our study. Furthermore, these samples are excellent for the study of long-range energy transfer between donor-acceptor binary systems. Our theoretical model is in excellent agreement with the experimental measurements both qualitatively and quantitatively.

## SUMMARY

We have completed a detailed study of the energy transfer between donor and acceptor systems via the Forster dipole-dipole interaction. Extension of our previous research<sup>24</sup> to a concentration dependence has confirmed our previous theory and has given us a more detailed description of energy loss of the donor with a strong or weak interaction with acceptors at different concentrations. We not only found a decrease of the relaxation decay time of the donors, but also observed a decrease in rise time of the acceptors in the presence of an increase of concentration of acceptors. Both indicate energy transfer. An important point to note is that the rise time of the acceptor does not match the decay time of the donor. Our theory fits the rise and decay time data well. This is the first study to measure the efficiency of energy transfer and present theoretical calculations for both donor and acceptors. Diffusion effects on the energy-transfer mechanism is under study at different viscosities and will be published in the near future.

## ACKNOWLEDGMENTS

We thank Y. Budansky for drawing the figures and N. Schiller of Hamamatsu for technical aid. This research was supported by NSF Energetics Engineering Program Grant No. 7920192, NASA Grant No. NAG-3-130, NIH Grant No. EY02515, and the AFOSR. The publication is supported by The City University Faculty Award Program.

- <sup>1</sup>K. B. Eisenthal and S. Siegal, *J. Chem. Phys.* **41**, 652 (1964).  
<sup>2</sup>R. G. Bennett, *J. Chem. Phys.* **41**, 3037 (1964).  
<sup>3</sup>S. A. Latt, H. T. Cheung, and E. R. Blout, *J. Am. Chem. Soc.* **87**, 995 (1965).  
<sup>4</sup>R. G. Bennett and R. E. Kellogg, *Photochem. and Photobiol.* **7**, 59 (1968).  
<sup>5</sup>K. B. Eisenthal, *Chem. Phys. Lett.* **6**, 155 (1970).  
<sup>6</sup>D. Rehm and K. B. Eisenthal, *Chem. Phys. Lett.* **9**, 387 (1971).

- <sup>7</sup>C. Lin and A. Dienes, *J. Appl. Phys.* **44**, 5050 (1973).  
<sup>8</sup>S. A. Ahmed, J. S. Gergely, and D. Infante, *J. Chem. Phys.* **61**, 1584 (1974).  
<sup>9</sup>R. W. Anderson, Jr., R. M. Hochstrasser, H. Lutz, and G. W. Scott, *J. Chem. Phys.* **61**, 2500 (1974).  
<sup>10</sup>T. Urisu and K. Kajiyama, *J. Appl. Phys.* **47**, 3563 (1976).  
<sup>11</sup>R. M. Hochstrasser and A. C. Nelson, *Chem. Phys. Lett.* **18**, 361 (1976).  
<sup>12</sup>R. Katraró, A. Ron, and S. Speiser, *Chem. Phys. Lett.*

- 52, 16 (1977).
- <sup>13</sup>Yu. I. Bukekov, S. A. Tikhomirov, G. B. Tolstorozhev, and D. M. Khalimanovich, *Kvant. Elektron. (Moscow)* **4**, 461 (1977) [*Sov. J. Quantum Electron.* **7**, 262 (1977)].
- <sup>14</sup>G. Porter and C. J. Tredwell, *Chem. Phys. Lett.* **56**, 278 (1978).
- <sup>15</sup>D. P. Millar, R. J. Robbins, and A. H. Zewail, *J. Chem. Phys.* **75**, 3649 (1981); M. C. Adams, D. J. Bradley, W. Sibbett, and J. R. Taylor, *Chem. Phys. Lett.* **66**, 428 (1979).
- <sup>16</sup>Th. Forster, *Ann. Phys. (Leipzig)* **2**, 55 (1948); *Discuss. Faraday Soc.* **27**, 7 (1959).
- <sup>17</sup>M. D. Galanin, *Zh. Eksp. Teor. Fiz.* **28**, 485 (1955) [*Sov. Phys.-JETP* **1**, 317 (1955)].
- <sup>18</sup>V. M. Korsunskii and A. N. Faidysh, *Opt. Spektrosk. Suppl.* **1**, 119 (1963) [*Opt. Spectrosc. (U.S.S.R.) Suppl.* **1**, 62 (1966)].
- <sup>19</sup>J. B. Birks, *Photophysics of Aromatic Molecules* (Wiley, New York, 1970).
- <sup>20</sup>R. G. Powell and Z. G. Soons, *J. Lumin.* **11**, 1 (1975).
- <sup>21</sup>A. Blumen and J. Manz, *J. Chem. Phys.* **71**, 4694 (1979).
- <sup>22</sup>J. Klafter and R. Siebey, *J. Chem. Phys.* **72**, 843 (1980).
- <sup>23</sup>K. Allinger and A. Blumer, *J. Chem. Phys.* **72**, 4608 (1980).
- <sup>24</sup>P. Y. Lu, Z. X. Yu, R. R. Alfano, and J. I. Gersten, *Phys. Rev. A* **26**, 3610 (1982).
- <sup>25</sup>P. Y. Lu, P. P. Ho, and R. R. Alfano, *IEEE J. Quantum Electron.* **QE-15**, 406 (1979).
- <sup>26</sup>N. H. Schiller, Y. Tsuchiya, E. Inuzuka, Y. Suzuki, K. Kinoshita, K. Kamiya, H. Iida, and R. R. Alfano, *Opt. Spectra* **14**, 55 (1980).
- <sup>27</sup>A. Penzkofer, W. Falkenstein, and W. Kaiser, *Chem. Phys. Lett.* **44**, 82 (1976).